PHYSICAL REVIEW C **69**, 041301(R) (2004)

Unmasking the nuclear matter equation of state

J. Piekarewicz
Department of Physics, Florida State University, Tallahassee, Florida 32306, USA
(Received 4 December 2003; published 5 April 2004)

Accurately calibrated (or "best fit") relativistic mean-field models are used to compute the distribution of isoscalar-monopole strength in ^{90}Zr and ^{208}Pb, and the isovector-dipole strength in ^{208}Pb using a continuum random-phase-approximation approach. It is shown that the distribution of isoscalar-monopole strength in ^{208}Pb—but not in ^{90}Zr—is sensitive to the density dependence of the symmetry energy. This sensitivity hinders the extraction of the compression modulus of symmetric nuclear matter from the isoscalar giant monopole resonance (ISGMR) in ^{208}Pb. Thus, one relies on ^{90}Zr, a nucleus with both a small neutron-proton asymmetry and a well developed ISGMR peak, to constrain the compression modulus of symmetric nuclear matter to the range $K=(248\pm 8)$ MeV. In turn, the sensitivity of the ISGMR in ^{208}Pb to the density dependence of the symmetry energy is used to constrain its neutron skin to the range $R_n - R_p \lesssim 0.22$ fm. The impact of this result on the enhanced cooling of neutron stars is briefly addressed.

DOI: 10.1103/PhysRevC.69.041301 PACS number(s): 24.10.Jv, 21.10.Re, 21.60.Jz

Constraining the equation of state (EOS) of neutron-rich matter remains a fundamental problem in nuclear physics and astrophysics. The stability of neutron-rich nuclei [1], the dynamics of heavy-ion collisions [2,3], the structure of neutron stars [4], and the simulation of core-collapse supernova [5,6], all depend sensitively on the EOS. Unfortunately, our window to the EOS is limited by terrestrial experiments that have, until now, probed stable nucleonic matter at (or close to) nuclear-matter saturation density. Fortunately, dramatic improvements are unfolding on several fronts. First, the commissioning of new radioactive-beam facilities all over the world will probe the EOS at large neutron-proton asymmetries. By defining the limits of nuclear existence, these exotic nuclei will constrain the EOS of neutron-rich matter at (and below) normal nuclear densities. Second, space-based telescopes have started to place important constraints on the high-density component of the EOS [7,8]. New telescopes operating at a variety of wavelengths are turning neutron stars from theoretical curiosities into powerful diagnostic tools.

The nuclear matter equation of state is conveniently parametrized in terms of the energy of symmetric nuclear matter ($\mathcal{B}/\mathcal{A}$) and the symmetry energy ($\mathcal{S}/\mathcal{A}$) in the following form:

$$\begin{aligned}\mathcal{E}/\mathcal{A}(k_F,b) - M &= \mathcal{B}/\mathcal{A}(k_F) + b^2\mathcal{S}/\mathcal{A}(k_F) + O(b^4)\\ &= \left(\varepsilon_0 + \frac{1}{2}K\xi^2 + \cdots\right)\\ &\quad + b^2\left(J + L\xi + \frac{1}{2}K_{\rm sym}\xi^2 + \cdots\right). \qquad (1)\end{aligned}$$

Here the deviation from the equilibrium Fermi momentum is denoted by $\xi \equiv (k_F - k_F^0)/k_F^0$, the neutron-proton asymmetry by $b \equiv (N-Z)/A$, and the various coefficients $(K, J, L, K_{\rm sym})$ parametrize the density dependence of the EOS around saturation density.

Seven decades of nuclear physics have placed important constraints on the nuclear matter equation of state. Indeed, the energy systematics of medium to heavy nuclei, when combined with accurately calibrated models, place the saturation point of symmetric nuclear matter at a density of $\rho_0 \simeq 0.15$ fm^{-3} ($k_F^0 \simeq 1.3$ fm^{-1}) and a binding energy per nucleon of $\varepsilon_0 \simeq -16$ MeV. It should be noted that one of the main virtues of the above Taylor-series expansion around saturation density [Eq. (1)] is that the linear term in ξ for symmetric nuclear matter (i.e., the pressure) automatically vanishes. Yet no such *special* saturation point exists in the case of the symmetry energy. Indeed, the symmetry energy at saturation density is not well known. Rather, it is the symmetry energy at the lower density of $\widetilde{\rho}_0 \simeq 0.10$ fm^{-3} ($\widetilde{k}_F^0 \simeq 1.15$ fm^{-1}) that seems to be accurately constrained (to within 1 MeV) by available ground-state observables [9,10]. It should be emphasized that present-day experiments can fix only one *isovector* quantity. If one insists—and one should not—on constraining the parameters of the symmetry energy at saturation density, then one would find a strong correlation among its parameters $(J, L, K_{\rm sym}, \ldots)$ [10]. For example, relativistic models consistently predict larger values for both the symmetry-energy coefficient J and the slope L at saturation density relative to nonrelativistic Skyrme models. This must be so if all models are to reproduce the value of the symmetry energy at the lower Fermi momentum of $\widetilde{k}_F^0$. Thus, in the present contribution we adopt the following convention: the symmetry energy is expanded around $\widetilde{k}_F^0 \simeq 1.15$ fm^{-1} and the value of the symmetry energy at $\widetilde{k}_F^0$ is fixed at $\widetilde{J} = 25.67$ MeV. That is,

$$\mathcal{S}/\mathcal{A}(k_F) = \widetilde{J} + \widetilde{L}\,\widetilde{\xi} + \tfrac{1}{2}\widetilde{K}_{\rm sym}\widetilde{\xi}^2 + \cdots, \qquad (2)$$

where $\widetilde{\xi} = (k_F - \widetilde{k}_F^0)/\widetilde{k}_F^0$. Note that henceforth "tilde" quantities refer to parameters of the symmetry energy at $\widetilde{k}_F^0 \simeq 1.15$ fm^{-1}.

Having established that existing ground-state observables accurately determine the binding energy per nucleon ε_0 at k_F^0 and the symmetry-energy coefficient $\widetilde{J}$ at $\widetilde{k}_F^0$, how can one

constrain any further the density dependence of the equation of state? In the case of symmetric nuclear matter, the dynamics of small density fluctuations around the saturation point is controlled by the compression modulus K. The isoscalar giant monopole resonance (ISGMR) in heavy nuclei has long been regarded as the optimal observable from which to determine the compression modulus [11]. This is especially true now that the *breathing mode* has been measured on a variety of nuclei with unprecedented accuracy [12]. In contrast, the density dependence of the symmetry energy is poorly constrained. Indeed, one may fit a variety of ground-state observables (such as charge densities, binding energies, and single-particle spectra) using accurately calibrated models that, nevertheless, predict a wide range of values for the neutron skin of ^{208}Pb [13]. As the neutron skin of a heavy nucleus is strongly correlated to the slope of the symmetry energy [9,10], measuring the skin thickness of a single heavy nucleus will constrain the density dependence of the symmetry energy. The Parity Radius Experiment at the Jefferson Laboratory aims to measure the neutron radius of ^{208}Pb accurately (to within 0.05 fm) and model independently via parity-violating electron scattering [14,15]. This experiment should provide a unique observational constraint on the density dependence of the symmetry energy.

While the above arguments suggest a clear path toward constraining the density dependence of the EOS, theoretical uncertainties have clouded these issues. First and foremost is the apparent discrepancy between nonrelativistic and relativistic predictions for the value of the compressional modulus of symmetric nuclear matter required to reproduce the ISGMR in ^{208}Pb. While nonrelativistic models predict $K \simeq 220-235$ MeV [16–18], relativistic models argue for a significantly larger value $K \simeq 250-270$ MeV [19–21]. Further, relativistic models systematically predict larger values for the neutron skin of ^{208}Pb relative to nonrelativistic Skyrme models. One of the goals of this contribution is to show that these two points are related. Indeed, the aim of this contribution is twofold. First, to vindicate—through the exclusive use of accurately calibrated models—our previous assertion that the distribution of ISGMR in heavy nuclei, and therefore the inferred value of K, is sensitive to the density dependence of the symmetry energy [22]. Second, to rely on existing data on the isoscalar giant-monopole resonance in ^{90}Zr and ^{208}Pb [12], and on the isovector giant-dipole resonance in ^{208}Pb [23], to set limits—simultaneously—on the compression modulus of symmetric nuclear matter and on the neutron skin of ^{208}Pb. Note that since first proposed [22], other groups have addressed the possible impact of the density dependence of the symmetry energy on the ISGMR in ^{208}Pb [21,24,25].

The starting point for the calculations is an interacting Lagrangian density of the following form [13,26]:

$$\mathcal{L}_{\rm int} = \bar{\psi}\left[g_{\rm s}\phi - \left(g_{\rm v}V_\mu + \frac{g_\rho}{2}\boldsymbol{\tau}\cdot\mathbf{b}_\mu + \frac{e}{2}(1+\tau_3)A_\mu \right)\gamma^\mu \right]\psi - \frac{\kappa}{3!}\Phi^3 - \frac{\lambda}{4!}\Phi^4 + \Lambda_{\rm v}(W_\mu W^\mu)(\mathbf{B}_\mu\cdot\mathbf{B}^\mu), \tag{3}$$

where $\Phi = g_{\rm s}\phi$, $W_\mu = g_{\rm v}V_\mu$, and $\mathbf{B}_\mu = g_\rho \mathbf{b}_\mu$. The Lagrangian density includes Yukawa couplings of the nucleon field to a scalar (ϕ) and to three vector (V^μ, $\mathbf{b}^\mu$, and A^μ) fields. In addition to the Yukawa couplings, the Lagrangian is supplemented by three nonlinear meson interactions. The inclusion of scalar-meson interactions (via κ and λ) is used to soften the equation of state of symmetric nuclear matter, while the mixed isoscalar-isovector coupling ($\Lambda_{\rm v}$) modifies the density dependence of the symmetry energy—without affecting well-known ground-state properties. Note that this last term was absent from Ref. [22], so the softening of the symmetry energy had to be done artificially. This drawback has now been corrected.

The relativistic mean-field models employed here are motivated by the enormous success of the NL3 parametrization [19]. For a detailed description of the fitting procedure used to calibrate the NL3 interaction and for its many successful predictions, we refer the reader to Ref. [27]. The NL3000 set used here (having $\Lambda_{\rm v}=0$) is practically identical to the original NL3 model. The other sets are obtained by adding an isoscalar-isovector coupling $\Lambda_{\rm v} \neq 0$, while at the same time readjusting the strength of the $NN\rho$ coupling constant (g_ρ) to maintain the symmetry-energy coefficient fixed at $\widetilde{J} = 25.67$ MeV (see discussion above). The values adopted for the isoscalar-isovector coupling range from $\Lambda_{\rm v}=0$ to $\Lambda_{\rm v}=0.04$. Introducing this extra model parameter enables one to adjust the poorly known density dependence of the symmetry energy and, in turn, the neutron skin of heavy nuclei. For example, the neutron-skin of ^{208}Pb ranges from $R_n - R_p = 0.28$ fm, for the set with the stiffest symmetry energy (NL3000), all the way down to $R_n - R_p = 0.17$ fm, for the softest parameter set (NL3040). Note that the label attached to the various parameter sets (NL3000, …, NL3040) reflects the value of the isoscalar-isovector coupling $\Lambda_{\rm v}$. For example, the parameter set NL3020 indicates that the Lagrangian density in Eq. (3) includes an isoscalar-isovector coupling constant equal to $\Lambda_{\rm v}=0.020$. The aim of this added coupling is to change the neutron density of heavy nuclei, while leaving intact ground-state observables that are well constrained experimentally. One should stress that the addition of $\Lambda_{\rm v}$ has no impact on the properties of symmetric nuclear matter, so the saturation properties remain unchanged. In summary, all the models used in this contribution share the following properties with the original NL3 model of Ref. [19]: for symmetric nuclear matter, a Fermi momentum at saturation of $k_F^0 = 1.30$ fm^{-1} with a binding energy per nucleon of $\varepsilon_0 = -16.24$ MeV, and a compression modulus of $K = 271$ MeV. For the symmetry energy, a symmetry-energy coefficient of $\widetilde{J} = 25.67$ MeV at a Fermi momentum of $\widetilde{k}_F^0 = 1.15$ fm^{-1}.

While the success of the NL3 interaction in reproducing ground-state properties (such as binding energies, charge radii, energy separations, etc.) for a variety of nuclei all throughout the periodic table is well documented, we display in Table I ground-state properties for only the two nuclei of relevance to this contribution, namely, ^{90}Zr and ^{208}Pb. Note that a center-of-mass correction equal to $\omega_{\rm c.m.} = (3/4)41A^{-4/3}$ has been applied to the binding energy per nucleon. However, even these accurately calibrated models

TABLE I. Binding energy per nucleon, root-mean-square charge radius, neutron-minus-proton root-mean-square radius, compression modulus for asymmetric ($b=0.111$ and) nuclear matter, and peak and centroid ISGMR energies for ^{90}Zr in the various models discussed in the text. The binding energy includes a center-of-mass correction of −0.08 MeV/nucleon, while the centroid energy m_1/m_0 (enclosed in square brackets) was computed by generating the distribution of strength in the range $10 \leqslant \omega \leqslant 26$ MeV. The second set of numbers in the table are for ^{208}Pb ($b=0.212$) with a center-of-mass correction of −0.02 MeV/nucleon and a centroid energy extracted from a distribution of strength generated in the range $8 \leqslant \omega \leqslant 23$ MeV. Experimental centroid energies extracted from Ref. [12].

Model	B/A (MeV)	$r_{\rm ch}$ (fm)	$R_n - R_p$ (fm)	K_b (MeV)	$E_{\rm ISGMR}[m_1/m_0]$ (MeV)
NL3000	8.69	4.26	0.11	263.13	18.10 [18.62]
NL3010	8.69	4.26	0.10	263.76	18.14 [18.67]
NL3020	8.70	4.26	0.09	265.23	18.15 [18.69]
NL3030	8.70	4.27	0.08	266.84	18.20 [18.75]
NL3040	8.70	4.27	0.07	268.32	18.25 [18.77]
Experiment	8.71±0.01	4.26±0.01	Unknown	Unknown	[17.89±0.20]
NL3000	7.87	5.51	0.28	242.93	14.35 [14.32]
NL3010	7.89	5.51	0.25	244.22	14.45 [14.43]
NL3020	7.91	5.51	0.22	248.88	14.62 [14.57]
NL3030	7.91	5.52	0.20	254.46	14.82 [14.74]
NL3040	7.92	5.53	0.17	259.87	15.03 [14.91]
Experiment	7.87±0.01	5.50±0.01	Unknown	Unknown	[14.24±0.11]

predict a wide range of values for the neutron skin of ^{208}Pb, confirming that the neutron skin of a heavy nucleus is not tightly constrained by known nuclear observables. The fifth column in the table displays the compression modulus of *asymmetric* nuclear matter with a neutron-proton asymmetry corresponding to ^{90}Zr ($b=0.111$) and ^{208}Pb ($b=0.212$). It is this quantity—not the compression modulus of symmetric nuclear matter—that is constrained by the breathing mode of nuclei. This simple fact makes the connection between the measured ISGMR and the compression modulus of *symmetric* nuclear matter sensitive to the density dependence of the symmetry energy. Recall that the compression modulus of symmetric nuclear matter was fixed in all models at $K=271$ MeV, yet for ($b=0.212$) asymmetric nuclear matter the compression modulus ranges from 243 MeV (for the stiffest symmetry energy) all the way up to 260 MeV (for the softest symmetry energy). Finally, the last column in the table shows peak and centroid energies for the ISGMR in ^{90}Zr and ^{208}Pb computed in a relativistic random-phase approximation (RPA). The distribution of isoscalar-longitudinal strength $S_L(q,\omega)$ from which the centroid energies have been extracted is displayed in Figs. 1 and 2, respectively. As expected, there is a strong correlation between the centroid energies and the compression modulus of *asymmetric* nuclear matter. One should note in passing that the continuum RPA formalism employed here, but reported elsewhere [28,29], respects important symmetries of nature, such as translational invariance (in the form of Thouless' theorem [30,31]) and the conservation of the vector current.

The great advantage of a nucleus such as ^{90}Zr is that it has both a well developed isoscalar-monopole peak and a small neutron-proton asymmetry ($b=0.111$). The latter manifests itself into the near collapse of all curves in Fig. 1 into a single one, so that the former may directly constrain the compression modulus of symmetric nuclear matter. In contrast to ^{90}Zr, *the distribution of ISGMR strength in* ^{208}*Pb is sensitive to the density dependence of the symmetry energy*. While this sensitivity should be sufficient to constrain the density dependence of the symmetry energy, one could do even better. Indeed, one may constrain the density dependence of the symmetry energy by demanding that both the ISGMR and the isovector giant-dipole resonance (IVGDR) in ^{208}Pb be simultaneously reproduced. The distribution of isovector-dipole strength in ^{208}Pb is displayed in Fig. 3. We note that the isovector-dipole response gets hardened as the

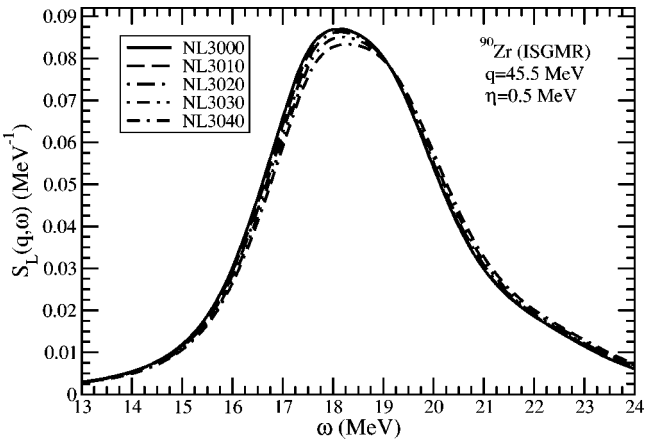

FIG. 1. Distribution of isoscalar-monopole strength in ^{90}Zr at a reference momentum transfer of $q=45.5$ MeV. The response includes a small artificial width of 0.5 MeV.

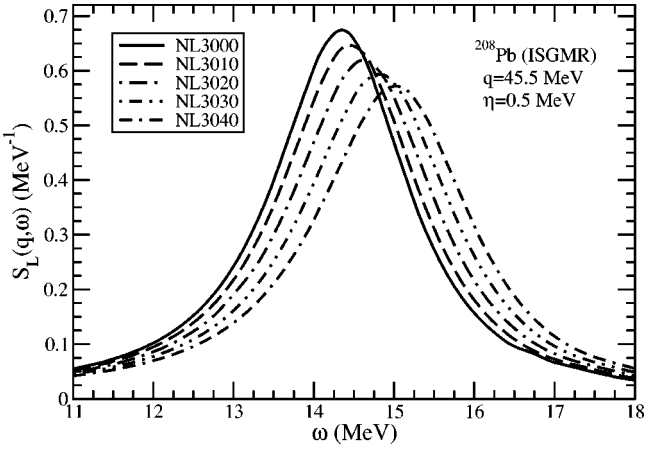

FIG. 2. Distribution of isoscalar-monopole strength in ^{208}Pb at a reference momentum transfer of $q=45.5$ MeV. The response includes a small artificial width of 0.5 MeV.

symmetry energy is softened. As all models share the same value of the symmetry-energy coefficient at $\tilde{k}_F^0=1.15$ fm^{-1}, the hardening of the response follows as a result of the symmetry energy being higher at the (low) densities relevant to the isovector-dipole mode [21].

To constrain simultaneously the compression modulus of symmetric nuclear matter and the neutron radius of ^{208}Pb, one starts by noticing that the theoretical centroid energy of the ISGMR in ^{90}Zr overestimates the experimental value by about 1 MeV . Although a proper adjustment of K should be done through a recalibration of parameters, a simple, yet accurate estimate may be obtained via the following scaling relation: $E_{\rm ISGMR}\propto\sqrt{K}$ [17]. Using this relation and accounting for experimental uncertainties, an adjustment of about 20 MeV in K is required to reproduce the ISGMR in ^{90}Zr. That is, $K=271$ MeV$\rightarrow K=(248\pm8)$ MeV. This adjustment in K induces a corresponding correction in the calculated values of the ISGMR in ^{208}Pb. The centroid energies after correction, together with the peak energies of the IVGDR in

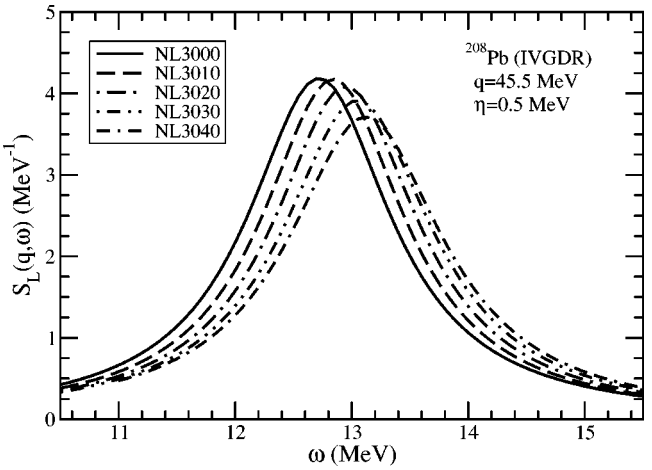

FIG. 3. Distribution of isovector-dipole strength in ^{208}Pb at a reference momentum transfer of $q=45.5$ MeV. The response includes a small artificial width of 0.5 MeV.

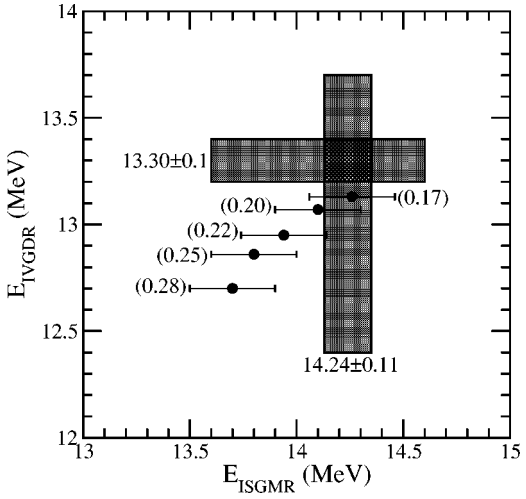

FIG. 4. Comparison between theoretical and experimental ISGMR centroid and IVGDR peak energies for ^{208}Pb. Quantities in parentheses represent the predictions for the neutron skin of ^{208}Pb in the various models discussed in the text.

^{208}Pb, are displayed in Fig. 4, alongside the experimental values [12,23]. The numbers in parentheses indicate the predicted values for the neutron skin in ^{208}Pb. The figure suggests that models with neutron skins in ^{208}Pb larger than $R_n-R_p\simeq0.22$ fm may have an unrealistically stiff symmetry energy.

In summary, relativistic mean-field models have been used to compute the distribution of isoscalar-monopole strength in ^{90}Zr and ^{208}Pb, and of isovector-dipole strength in ^{208}Pb using a continuum RPA approach. It was demonstrated—using exclusively accurately calibrated models—that the distribution of isoscalar-monopole strength in ^{208}Pb is sensitive to the density dependence of the symmetry energy. Further, existing experimental data were used to set limits on both the compression modulus of symmetric nuclear matter and on the neutron skin of ^{208}Pb. It appears that medium-mass nuclei having a well-developed ISGMR peak and a small neutron-proton asymmetry (such as ^{90}Zr but not ^{208}Pb) allow for the best determination of the compression modulus of symmetric nuclear matter. In turn, the sensitivity of the ISGMR and the IVGDR in ^{208}Pb to the density dependence of the symmetry energy may be used to impose constraints on the neutron skin of ^{208}Pb. From the present analysis, a compression modulus of $K=(248\pm8)$ MeV and a neutron skin in ^{208}Pb of $R_n-R_p\lesssim0.22$ fm were obtained. These values appear closer to those predicted in nonrelativistic studies. Further, it is also gratifying to see that the gap narrows among seemingly distinct relativistic models. Indeed, having adjusted the compression modulus to $K=(248\pm8)$ MeV, the NL3040 parameter set suggests the following values for three essential observables in ^{208}Pb: a neutron skin of $R_n-R_p=0.17$ fm, a centroid ISGMR energy of $E_{\rm ISGMR}=14.2\pm0.2$ MeV, and a peak IVGDR energy of $E_{\rm IVGDR}=13.1$ MeV. These values should be compared to the recent predictions by Vretenar, Niksić, and Ring using an accurately calibrated model containing density-dependent coupling constants [21]. Using a compression modulus of $K=250$ MeV, they obtain a neutron skin of R_n-R_p

$\simeq 0.175$ fm, a centroid ISGMR energy of $E_{\mathrm{ISGMR}} \simeq 13.9$ MeV, and a centroid—*not peak*—IVGDR energy of $E_{\mathrm{IVGDR}} \simeq 13.6$ MeV.

We conclude with a comment on the impact of these results on the cooling of neutron stars. In earlier publications we have demonstrated how improved values for neutron radii could have a widespread impact on the structure and dynamics of neutron stars [13,26,32,33]. In particular, we suggested that the enhanced cooling of the neutron star in 3C58 [34] may be due to the conventional URCA process—provided the symmetry energy is stiff enough to generate a neutron skin in ^{208}Pb larger than $R_n - R_p \gtrsim 0.24$ fm. In view of our present findings, this now seems unlikely. Thus, the possibility that 3C58 harbors an exotic star, such as a quark star, looms large.

The author is grateful to the organizers of the International Workshop on "Nuclear Response under Extreme Conditions" in Trento and to the ECT* for their support and hospitality. This work was supported in part by the U.S. Department of Energy under Contract No. DE-FG05-92ER40750.

[1] B. Todd and J. Piekarewicz, Phys. Rev. C **67**, 044317 (2003).
[2] P. Danielewicz, R. Lacey, and W. G. Lynch, Science **298**, 1592 (2002).
[3] B.-A. Li, Phys. Rev. Lett. **88**, 192701 (2002), and references therein.
[4] J. M. Lattimer and M. Prakash, Astrophys. J. **550**, 426 (2001), and references therein.
[5] K. Sumiyoshi, H. Suzuki, and H. Toki, Astron. Astrophys. **303**, 475 (1995).
[6] R. Buras, M. Rampp, H. T. Janka, and K. Kifonidis, Phys. Rev. Lett. **90**, 241101 (2003), and references therein.
[7] J. A. Pons, F. M. Walter, J. M. Lattimer, R. Prakash, M. Neuhauser, and P.-H. An, Astrophys. J. **564**, 981 (2002), and references therein.
[8] F. M. Walter and J. M. Lattimer, Astrophys. J. Lett. **576**, L145 (2002).
[9] B. A. Brown, Phys. Rev. Lett. **85**, 5296 (2000).
[10] R. J. Furnstahl, Nucl. Phys. **A706**, 85 (2002).
[11] J. P. Blaizot, Phys. Rep. **64**, 171 (1980).
[12] D. H. Youngblood, H. L. Clark, and Y. W. Lui, Phys. Rev. Lett. **82**, 691 (1999).
[13] C. J. Horowitz and J. Piekarewicz, Phys. Rev. Lett. **86**, 5647 (2001).
[14] C. J. Horowitz, S. J. Pollock, P. A. Souder, and R. Michaels, Phys. Rev. C **63**, 025501 (2001).
[15] R. Michaels, P. A. Souder, and G. M. Urciuoli, spokespersons, Jefferson Laboratory Experiment E00–003.
[16] G. Colò, P. F. Bortignon, N. Van Gai, A. Bracco, and R. A. Broglia, Phys. Lett. B **276**, 279 (1992).
[17] J. P. Blaizot, J. F. Berger, J. Dechargé, and M. Girod, Nucl. Phys. **A591**, 435 (1995).
[18] I. Hamamoto, H. Sagawa, and X. Z. Zhang, Phys. Rev. C **56**, 3121 (1997).
[19] G. A. Lalazissis, J. Konig, and P. Ring, Phys. Rev. C **55**, 540 (1997).
[20] D. Vretenar, A. Wandelt, and P. Ring, Phys. Lett. B **487**, 334 (2000).
[21] D. Vretenar, T. Niksić, and P. Ring, Phys. Rev. C **68**, 024310 (2003).
[22] J. Piekarewicz, Phys. Rev. C **66**, 034305 (2002).
[23] J. Ritman *et al.*, Phys. Rev. Lett. **70**, 533 (1993).
[24] B. K. Agrawal, S. Shlomo, and V. Kim Au, Phys. Rev. C **68**, 031304 (2003).
[25] G. Colò and N. Van Gai, nucl-th/0309002
[26] C. J. Horowitz and J. Piekarewicz, Phys. Rev. C **64**, 062802(R) (2001).
[27] G. A. Lalazissis, S. Raman, and P. Ring, At. Data Nucl. Data Tables **71**, 1 (1999).
[28] J. Piekarewicz, Phys. Rev. C **62**, 051304(R) (2000).
[29] J. Piekarewicz, Phys. Rev. C **64**, 024307 (2001).
[30] D. J. Thouless, Nucl. Phys. **22**, 78 (1961).
[31] J. F. Dawson and R. J. Furnstahl, Phys. Rev. C **42**, 2009 (1990).
[32] C. J. Horowitz and J. Piekarewicz, Phys. Rev. C **66**, 055803 (2002).
[33] J. Carriere, C. J. Horowitz, and J. Piekarewicz, Astrophys. J. **593**, 463 (2003).
[34] P. Slane, D. J. Helfand, and S. S. Murray, Astrophys. J. Lett. **571**, L45 (2002).